

# HIGH STABILITY UHF OSCILLATORS USING A SUPERCONDUCTING CAVITY

F. Biquard, Nguyen Tuong Viet, and A. Septier  
Institut d'Electronique Fondamentale  
Orsay, France

## I. INTRODUCTION

The recent achievement of very high Q factors in superconducting cavities makes possible the realization of powerful microwave oscillators with natural frequency stability as good as that of quartz clocks. This interesting property is a consequence of the Blaquièrre-Townes<sup>1</sup> formula giving the noise bandwidth of a slightly nonlinear oscillator influenced by Johnson noise as:

$$\delta f = \pi k T \frac{(\Delta f)^2}{P} \quad (1)$$

where  $\Delta f$  denotes the bandwidth of the oscillating circuit and P the microwave power in the circuit.

A superconducting cavity can be used as a part of an oscillator in many ways; we present here two different systems in which the cavity plays, respectively, the role of an active or passive component.

### 1. Monotron

In the monotron oscillator an electron beam is able to transfer a part of its energy to the electromagnetic field in a resonant cavity. Regions of negative conductance appear in the beam loading characteristics of the beam-cavity system, suggesting the possibility of regenerative operation. A general theory of the monotron oscillator has been first given by Muller and Rostas<sup>2</sup> and then by Turner.<sup>3</sup> It turns out that the performance of monotron oscillators can be described correctly in terms of the lumped equivalent circuit shown in Fig. 1, where the admittance  $G_b + j B_b$  represents the effect of the electron beam on the equivalent circuit of the cavity.

In this case the main source of noise is shot noise from the electron beam which is  $10^8$  greater than Johnson noise for a typical case. Replacing Johnson noise power in the cavity,  $P_j = 4kT\Delta f$ , by shot noise coming from the electron beam,  $P_s = M^2 e I_0 \Delta f / G_c$ , and following the Golay<sup>4</sup> method, we find that the effect of noise is adequately described in first approximation by a noise bandwidth  $\delta f$ ,  $\delta f$  being given by:

$$\delta f = \frac{2\pi M^2 e I_0}{G_c} \frac{f^2}{Q} \frac{1}{P} \quad (2)$$

- 
1. A. Blaquièrre, Thèse Paris, Gauthiers Villars, 1953;  
J.P. Gordon, H.J. Zeiger, and C.H. Townes, Phys. Rev. 99, 1264 (1955).
  2. J.J. Muller and E. Rostas, Helv. Phys. Acta 13, 435 (1940).
  3. C.W. Turner, Stanford University Report 830 (1961).
  4. M.J.E. Golay, Proc. IRE 48, 1473 (1960).

where

- $I_o$  = dc beam current crossing the cavity, (A),  
 $G_c$  = shunt admittance of the cavity, ( $\Omega^{-1}$ ),  
 $D$  = transit angle of electrons through the cavity, (rad),  
 $M = \frac{\sin D/2}{D/2}$  = gap coupling coefficient,  
 $f$  = frequency of oscillation, (Hz),  
 $Q$  = quality factor of the cavity,  
 $P$  = microwave power delivered to the circuit, (W).

In the same conditions, the relative standard deviation<sup>5</sup> of the frequency in time  $\tau$  is given by:

$$\frac{\sigma(\langle \dot{\phi} \rangle_{t,\tau})}{2\pi f} = \left( \frac{M^2 e I_o}{8 G_c Q^2 \tau} \right)^{\frac{1}{2}} \quad (3)$$

For an oscillator using a cylindrical cavity working in the  $TM_{010}$  mode, in the best conversion efficiency conditions ( $D = 2.33 \pi$ ), formulas (2) and (3) take the form:

$$\delta f = 2 \times 10^{-14} \frac{f^2}{Q^2 P} \quad (4)$$

$$\frac{\sigma(\langle \dot{\phi} \rangle_{t,\tau})}{2\pi f} = 2.8 \times 10^{-9} \left( \frac{1}{P Q^2 \tau} \right)^{\frac{1}{2}} \quad (5)$$

Choosing a working frequency of 3 GHz, we could use a cavity having  $Q = 10^7$ . The oscillator may conveniently deliver 0.1 W of microwave power, and the noise bandwidth is then:

$$\delta f = 1.8 \times 10^{-8} \text{ Hz}$$

with

$$\delta f/f = 6 \times 10^{-18} \quad (6)$$

## 2. TWT Oscillator

In the traveling wave tube (TWT) auto-oscillator, the cavity is placed in the external feedback loop of a low noise TWT amplifier to play the role of a frequency-determining circuit. The problem of noise in this type of oscillator has been discussed in detail by Hetland.<sup>6</sup> To compute the noise bandwidth, one can consider the case

5. L.S. Cutler and C.L. Searle, Proc. IEEE 54, 136 (1966).

6. G. Hetland, Stanford University, Applied Electronics Laboratory Report No. 40 (1955).

of classical auto-oscillators. When introducing the noise factor and the power gain of the tube, it is possible to derive from the above Blaquiè-re-Townes formula the following expression for the noise bandwidth of the oscillator output spectrum:

$$\delta f = \frac{\pi k T_o F G f^2}{P Q^2} \quad (7)$$

where

- $\delta f$  = bandwidth of output spectrum, (Hz),
- $k$  = Boltzmann's constant, ( $1.37 \times 10^{-23}$  J/°K),
- $T_o$  = room temperature,
- $F$  = noise factor of the TWT at  $f$ ,
- $G$  = power gain of the TWT at  $f$ ,
- $P$  = output power, (W),
- $Q$  = quality factor of the cavity.

In fact, Eq. (7) defines the width of the Fourier spectrum, calculated in principle by integrals running from  $t = -\infty$  to  $t = \infty$ . In practice, we measure  $\delta f$  during a finite observation time  $\tau$  and we have<sup>7</sup>:

$$\delta f_{\tau} = \left( \frac{\delta f}{2\pi \tau} \right)^{\frac{1}{2}} \quad (8)$$

In the same conditions, the standard deviation of the frequency is given by:

$$\frac{\sigma(\langle \dot{\phi} \rangle_{t,\tau})}{2\pi f} = \left( \frac{k T_o F G}{2 P Q^2 \tau} \right)^{\frac{1}{2}} \quad (9)$$

For  $f = 2.911 \times 10^9$  Hz,  $F = 4.67$  (6.7 dB),  $G = 159$  (22 dB),  $P = 10^{-3}$  W,  $Q = 10^8$  we have:

$$\delta f = 8 \times 10^{-12} \text{ Hz}$$

$$\frac{\delta f}{f} = 2.7 \times 10^{-21}$$

$$\frac{\sigma(\langle \dot{\phi} \rangle_{t,\tau})}{2\pi f} = 1.2 \times 10^{-16} \text{ with } \tau = 10 \text{ sec.}$$

---

7. P. Grivet and A. Blaquiè-re, in Proc. Symposium on Optical Masers, Brooklyn, 1963, p. 69.

### 3. Comparison Between Oscillators

Table I shows theoretical properties of both oscillators in comparison with the properties of hydrogen and ammonia masers.

TABLE I

	TWT auto-oscillator	Quartz oscillator	Hydrogen maser	Ammonia maser	Monotron
$f_o$ (MHz)	2911	5	1420	23 870	3000
P (W)	$10^{-3}$	$10^{-7}$	$10^{-12}$	$10^{-10}$	$10^{-1}$
Q	$10^8$	$2 \times 10^6$	$2 \times 10^9$	$5 \times 10^6$	$10^7$
$\delta f$ (Hz)	$8 \times 10^{-12}$	$2.7 \times 10^{-12}$	$6.5 \times 10^{-9}$	$3 \times 10^{-3}$	$1.8 \times 10^{-8}$
$\delta f/f$	$2.7 \times 10^{-21}$	$0.54 \times 10^{-18}$	$4.7 \times 10^{-18}$	$1.25 \times 10^{-13}$	$6 \times 10^{-18}$
$\frac{\sigma (\langle \dot{\phi} \rangle_{t,T})}{2\pi f}$ $\tau = 10 \text{ sec}$	$1.2 \times 10^{-16}$	$4.2 \times 10^{-14}$	$7 \times 10^{-15}$	$2.9 \times 10^{-13}$	$3 \times 10^{-16}$

We can foresee that, for both oscillators, frequency stability will not be limited by noise bandwidth but by external factors. Particularly, long-term frequency stability will be influenced by a possible drift of the cavity resonance frequency caused by gas pressure variations in the helium bath.

## II. MONOTRON OSCILLATOR

### 1. Description

An electron beam of velocity  $u_o$  and intensity  $I_o$ , accelerated under a voltage  $V_o$ , flows along the axis of a cylindrical cavity of length  $d$ , oscillating at a frequency  $f$  in the  $TM_{0pq}$  mode. The electron beam exchanges power with the high frequency field in the cavity. If the transit angle of the electrons

$$D = \frac{2\pi f d}{u_o} \quad (10)$$

is well chosen, power can be delivered by the beam to the electromagnetic field and an oscillation can arise in the cavity.

For the  $TM_{010}$  mode (neglecting end perturbations caused by axial holes), the electric field  $E_z$  is uniform along the axis of the cavity and the oscillation condition

is found to be  $D = (2K + \frac{1}{2})\pi$ , K being an integer, but other oscillation modes are possible.

The cylindrical cavity resonates in the S band near  $f = 3$  GHz. Our cavities are made of OFHC copper and their inner surfaces are covered with a vacuum deposited or electrolytic thick lead layer (thickness of the order 5  $\mu\text{m}$ ).

Lead is a type I superconductor for temperatures  $T < 7.2^\circ\text{K}$ , and the devices were mainly operated at  $T = 4.2^\circ\text{K}$ . In this first realization (Fig. 2), the cavity is made in two identical pieces, the whole cavity being cut along a plane perpendicular to its axis. This solution is mechanically convenient, but it is a rather bad one from an electrical point of view. Indeed, the indium joint separating the two halves of the cavity causes supplementary H.F. losses, and the Q reached practically is not higher than  $10^7$  on the average.

Two holes 6 mm in diameter bored in the end plates allow the electron beam to cross the cavity along its axis. The resonant cavity, which is fixed in a special cryostat, constitutes the inner wall of the liquid helium vessel which is surrounded by a copper sheet. This sheet is soldered to four liquid nitrogen reservoirs and reduces radiative heat losses. Two coaxial lines fitted with movable antennas permit variation of the coupling between the cavity and the electrical external circuit at room temperature.

A triode electron gun with a tungsten wire cathode produces the electron beam which is focused by an electrostatic lens; 95% of the electrons reach the collector situated 30 cm from the cathode.

## 2. Properties of the Superconducting Monotron

Steady-state properties. Figure 3 gives experimental curves showing the starting current of the oscillator as a function of accelerating voltage for various oscillating modes of the cavity. We easily obtain oscillations in three different modes, and we give in Table II the measured characteristics of the oscillator.

TABLE II ( $d = 38$  mm)

	$\text{TM}_{010}$	$\text{TM}_{011}$	$\text{TM}_{020}$
Frequency (GHz)	2.970	4.956	6.817
Q factor	$12.25 \times 10^6$	$7.49 \times 10^6$	$10.2 \times 10^6$
Optimum transit angle (radians)	$4.5 \pi$ $6.5 \pi$	$5.5 \pi$	$8.5 \pi$
Optimum accelerating voltage (kV)	7.8 3.5	15	11.9

It is interesting to use modes like  $\text{TM}_{020}$  or  $\text{TM}_{011}$ , in order to reach higher frequencies of operation with the same resonator (X band, for example).  $\text{TM}_{011}$  modes are very promising if we need a high Q factor at high frequency because the joint in the

lateral wall of the cavity does not disturb the electric current pattern.

From a theoretical point of view it should appear interesting to study the competition between two possible modes for given experimental conditions.

Figure 4 shows theoretical and experimental curves giving the values of the starting current  $I_s$  of the oscillator operating in the  $TM_{010}$  mode, as a function of transit angle, the loaded Q factor being  $2.22 \times 10^6$ . We obtain a good agreement between experiment and theory, if we take into account the fact that theory neglects the action on the beam of the evanescent modes existing in the holes at each end of the cavity (the field repartition along the axis is supposed to be rectangular). More elaborate calculations taking into account the real shape of the leakage field configuration are in progress.

For a given transit angle D, we have checked that the product ( $Q \times I_s$ ) is a constant of the oscillator.

Long-term frequency stability. Figure 5 presents a record of monotron frequency variations during 21 minutes. Experimental working conditions are in this case:

Mode	$TM_{010}$
Loaded Q	$Q_L = 10^7$
Accelerating voltage	$V_o = 7.987$ kV
Beam current	$I_o = 1.25$ mA
Transit angle	$D = 4.30 \pi$
Helium bath temperature	$T = 4.2^{\circ}K$
Output power	$P = 0.15$ W
Sampling time	$\tau = 10$ sec

Stability of the accelerating voltage is better than 0.01%. We have measured the mean frequency  $f_M = 2969990106.05$  Hz and the mean square value of the error  $\bar{\sigma} = 0.66$  Hz.

The frequency stability is given by:

$$\sigma (\langle \dot{\varphi} \rangle_{t,\tau}) / 2\pi f = 2.2 \times 10^{-10} \quad (11)$$

for  $\tau = 10$  sec. On the same figure we present measurements on short-term frequency stability.

Possible factors governing residual frequency drifts. Two main factors may be of importance for explaining residual frequency instabilities.

- a) These instabilities may be caused by the electron beam accelerating voltage and current fluctuations. Theory shows that:

$$\frac{df}{f} = \frac{1}{Q} \left( \frac{D-1}{4} \frac{dV_o}{V_o} - \frac{1}{2} \frac{dI_o}{I_o} \right) \quad (12)$$

Instability of frequency due to this cause is inversely proportional to Q. Expectation values for  $dV_o$  and  $dI_o$  are:

$$\frac{d V_o}{V_o} \approx \frac{d I_o}{I_o} \approx 10^{-4} \quad (13)$$

and with an experimental  $Q = 10^7$ , formula (9) gives:

$$\frac{df}{f} \approx 10^{-11} \quad (14)$$

- b) A temperature variation  $\Delta T$  of the liquid helium bath induces a slow drift of the cavity resonant frequency. Indeed, the pressure  $P$  is not yet stabilized and for slow fluctuations the temperature changes with the pressure of the helium gas.

Temperature variations have three different effects:

- i) Thermal expansion of the cavity dimensions; at very low temperatures and for copper walls, this effect is negligible.
- ii) Variations of the surface reactance of the superconductor.
- iii) Mechanical deformation of the cavity walls due to external pressure variations.

In the vicinity of  $T = 4.2^{\circ}\text{K}$ , adding all preceding effects, we obtain an approximate value of frequency variation:

$$\frac{df}{f} \approx 1.5 \times 10^{-10} \times \Delta P/\text{Torr}$$

where  $P$  is the helium gas pressure in the cryostat.

The limit of useful power. It is possible to increase power from milliwatts to several watts by raising the beam current intensity above the threshold value. However, in order to maintain the frequency stability we are confined by two imperatives:

- a) Beam current has to be sufficiently weak so that it can be well focused and led across the cavity without losses on the walls, thus avoiding local heating of the metal surface.
- b) It is also necessary that high frequency losses in the cavity walls be kept small.

Indeed, too much thermal dissipation in the walls will cause boiling of the liquid helium and thus an elevation of temperature which shifts the oscillator frequency at a rate greater than 20 Hz/min. It has been proven that such "cryogenic" effects limit such an oscillator to an output power of 1 W if the highest frequency stability is required.

#### Short-term frequency stability.

- a) Method of measurement and results:- The short-term frequency stability has been determined by direct comparison with a stable 5 MHz oscillator followed by a multiplying chain to 2910 MHz. The stability of the reference chain is  $9 \times 10^{-13}$  for a 10 sec averaging time and  $6 \times 10^{-11}$  for a 0.01 sec averaging time. Each experimental point on the short-term frequency stability curve (Fig. 5) represents

the relative standard deviation of the frequency  $\sigma(\langle\dot{\phi}\rangle_{t,\tau})$  of a group of 800 measurements which have been treated in order to eliminate the slow drift coming from the liquid helium bath. In this way, we could evaluate the stability limit defined by (11) as reaching  $2 \times 10^{-10}$  for  $\tau > 0.1$  sec.

- b) Influence of the Q factor:- Several measurements of the short-term frequency stability were made using the same cavity, and varying the Q factor from  $1.66 \times 10^6$  to  $10.1 \times 10^6$ . The experimental results were always in accord with those of Fig. 5 without any noticeable difference, which seems to show that at the present time frequency stability does not depend on Q.
- c) Multipactor effect:- We think that a new phenomenon, not considered above, actually limits the frequency stability of the monotron. We are presently inclined to suppose that field electron emission from cavity walls can be such a possible source of noise. Indeed, high electric field strengths are obtained in the superconducting cavity ( $E > 10^6$  MV/m on the axis). If we still increase the field strength (by raising the beam current) multipactoring effects appear and oscillation vanishes and reappears again as a relaxation process.

These phenomena are especially troublesome in lead electroplated cavities, the lead surface being very rough; sharp crystal corners (visible on relatively low magnification micrographs) enhance the local electric field. The multipactor effect does not appear so easily (even at higher field strength) in cavities where the lead layer is obtained by vacuum deposition. In this case the surface presents better aspect and smoothness. Unfortunately, we are actually unable to obtain Q values higher than  $2.6 \times 10^6$  by this technique. New experiments are now in progress, using a new cavity, lead-plated by an ultra-high-vacuum deposition technique.

### III. TWT AUTO-OSCILLATOR

#### 1. Principle

Figure 7 shows the well-known block diagram of the oscillator.<sup>8,9</sup> A superconducting cavity is introduced in the external feedback loop of a TWT. The loop includes also a variable attenuator and a phase shifter for the purpose of adjusting gain and phase. The device can oscillate if the over-all gain is higher than unity and if the total phase shift is a multiple of  $2\pi$ .

Instabilities in the electrical length of the loop as well as mechanical vibrations, limit the observed frequency stability, but the use of a high Q superconducting cavity is highly efficient in reducing the resulting line width to a low value.

Here, the cavity is made of OFHC copper covered with a lead layer of about  $5 \mu$  in thickness. The oscillating mode is  $TE_{011}$  and the resonance frequency 2911 MHz. External coupling is secured by two small loops of coaxial lines. The resonance frequency is mechanically tunable between the limits  $2911 \pm 10$  MHz. A fine adjustment is provided by a superconducting lead plunger (Fig. 8).

---

8. M.S. Khaikin, Instr. and Experimental Techniques (transl.) 4, 518 (1961).

9. Nguyen Tuong Viet, Compt. Rend. Paris 258, 4218 (1964).

## 2. Frequency Stability

As shown in a previous paper<sup>10</sup> stability is controlled by the helium bath temperature, the room temperature and the high dc voltage applied to the helix of the TWT.

Helium bath temperature fluctuations are due to variations of the pressure of helium vapor; pressure could be well regulated and the temperature can be maintained constant within  $3 \times 10^{-5}$  °K at 2.1°K. Temperature fluctuations cause a change in the surface reactance of the superconductor and in the mechanical dimensions of the cavity (thermal expansion and elastic deformation due to pressure difference between the inside and the outside of the cavity). In any case they result in a slow drift of the resonance frequency.

A great part of the electrical circuit is at room temperature and subject to its variations, which change both mechanical length and dielectric permittivity. Standard precautions are enough to reduce the level of this kind of disturbance to a low level.

Another source of instabilities can arise from fluctuations of the dc voltage applied to the helix of the TWT which change the phase in the loop. The dc voltage used has a relative variation smaller than  $1.5 \times 10^{-5}$ .

Table III shows the frequency fluctuation  $df/f$  obtained by calculation.

TABLE III

TWT CSF/F4107B,  $T = 2.1^{\circ}\text{K}$ ,  $Q = 3.3 \times 10^7$

		<u>df/f</u>	
Helium bath temperature $ \Delta T  = 3 \times 10^{-5}$ °K	{	Thermal expansion	$1.3 \times 10^{-14}$
		Elastic deformation	$2 \times 10^{-11}$
		Surface reactance	$1.2 \times 10^{-13}$
Room temperature $ \Delta T  = 0.1^{\circ}\text{C}$	{	Coaxial length	$6.7 \times 10^{-12}$
		Permittivity (teflon)	$2.4 \times 10^{-11}$
Helix voltage $ dV/V  = 1.5 \times 10^{-5}$			$2.2 \times 10^{-11}$

Frequency fluctuations due to elastic deformation are difficult to reduce for given variations of helium bath temperature, even for higher Q of the cavity. But fluctuations due to room temperature changes and helix voltage variations can be made as small as possible by increasing Q (we have realized a cavity having a Q of  $3.3 \times 10^9$  at 2°K but higher Q's have been obtained at Stanford<sup>11</sup> and Brookhaven<sup>12</sup>).

10. Nguyen Tuong Viet, Ann. Phys. (Paris) 2, 225 (1967).

11. J.P. Turneure, Ph.D. Thesis, Stanford University Report HEPL 507 (1967).

12. H. Hahn, H.J. Halama, and E.H. Foster, J. Appl. Phys. 39, 2606 (1968).

### 3. Experiments Performed

#### Long-term frequency stability.

One milliwatt oscillator (TWT CSF/F4107B):

Figure 9 shows the measured frequency vs time for a 1 mW oscillator having the following parameters:

$$P = 1 \text{ mW}, f = 2911 \text{ MHz}, Q_L = 3.3 \times 10^7, T = 2.1 \pm 3 \times 10^{-5} \text{ }^\circ\text{K}, \\ dV/V = 1.5 \times 10^{-5} \text{ per minute.}$$

Over 6 minutes, the frequency changes by 0.8 Hz and the corresponding stability is  $2.7 \times 10^{-10}$ , i.e.,  $4.5 \times 10^{-11}$  per minute.

Figure 10 shows the influence of helium bath temperature on stability.

One watt oscillator (TWT Huggins HA100C):

In the 1 W oscillator, we have obtained a stability of  $3.4 \times 10^{-10}$  per minute under the following conditions:

$$P = 1 \text{ W}, f = 2911 \text{ MHz}, Q = 4 \times 10^7, T = 1.9 \pm 3 \times 10^{-4} \text{ }^\circ\text{K}, \\ dV/V = \pm 5 \times 10^{-4}.$$

Short-term frequency stability. To have an idea about the short-term frequency stability, the two output signals of the above oscillators are mixed to produce a beat signal whose average frequency is much lower than that of the input signals. The 12 MHz beat signal is mixed again with a frequency synthesizer, whose frequency fluctuations do not degrade the measurement, to get a low frequency signal of 10 kHz. The period of the latter is then measured by a counter and each measurement printed out in a digital recorder. The relative standard deviation of the frequency  $\sigma(\langle \dot{\phi} \rangle_{t, \tau})/2\pi f$  is calculated for different values of  $\tau$ . Figure 11 illustrates the results obtained after removal of slow drifts.

### IV. CONCLUSION

We hope that better long-term stabilities will be obtained in the monotron oscillator after a stabilization of the liquid helium bath temperature; some improvements on voltage source regulation also appear now feasible.

It seems possible to obtain with these oscillators frequency stability as good as that of the best quartz multiplier sets, retaining the advantages of relatively high power and frequency adjustment (in the TWT oscillator).

Much higher frequencies can also be explored, and new experiments are going in this way: in the monotron oscillator, the modulated beam emerging from the superconducting cavity tuned at  $f_0$  is forced to cross a second cavity, resonating at a harmonic frequency  $nf_0$ , and power can be obtained at this frequency.

In the future, one-cavity linear accelerators could be powered by using a high-power amplifier and the accelerator cavity itself.

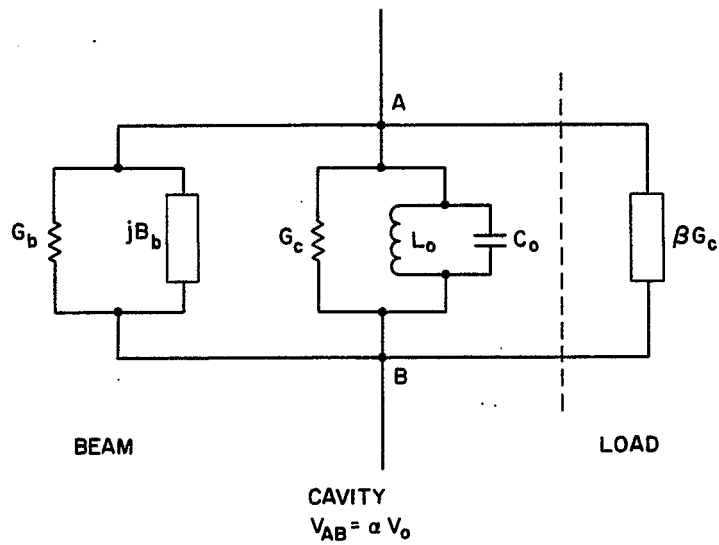


Fig. 1. Equivalent circuit of the monotron.

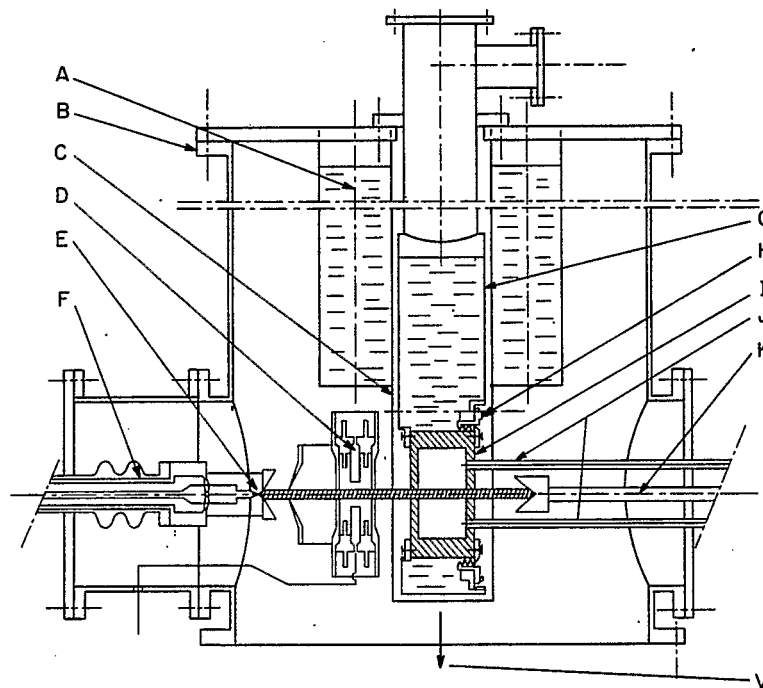


Fig. 2. Arrangement for monotron with superconducting cavity: A, liquid nitrogen vessel; B, vacuum chamber; C, copper sheet; D, electrostatic lens; E, triode electrode gun; F, high voltage isolation of the electron gun; G, liquid helium vessel; H, indium gasket for vacuum; I, superconducting cavity; J, coupling coaxial guide; K, electron collector; V, vacuum pump.

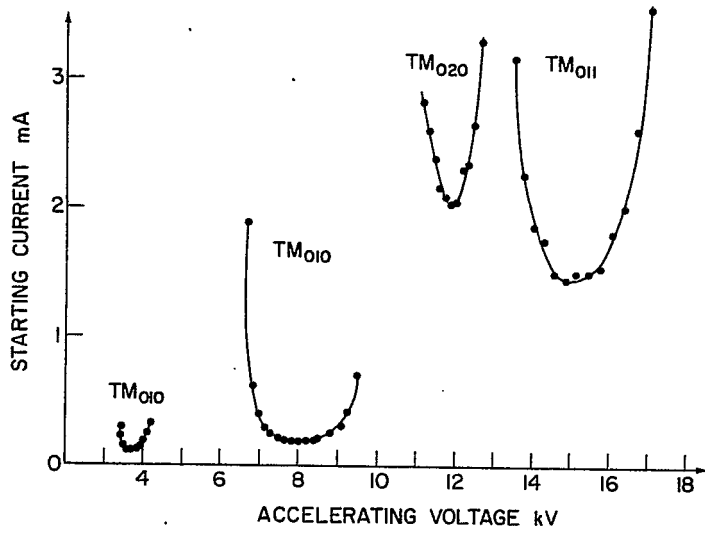


Fig. 3. Starting current in various oscillation modes in cavity with  $Q = 10^7$ .

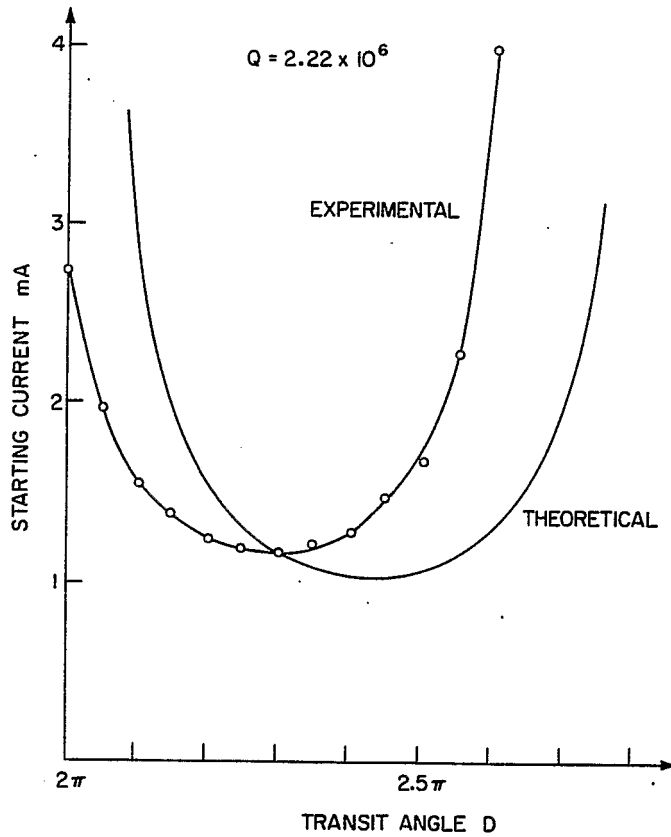


Fig. 4. Starting current of oscillation in  $TM_{010}$  mode at  $Q = 2.22 \times 10^6$ .

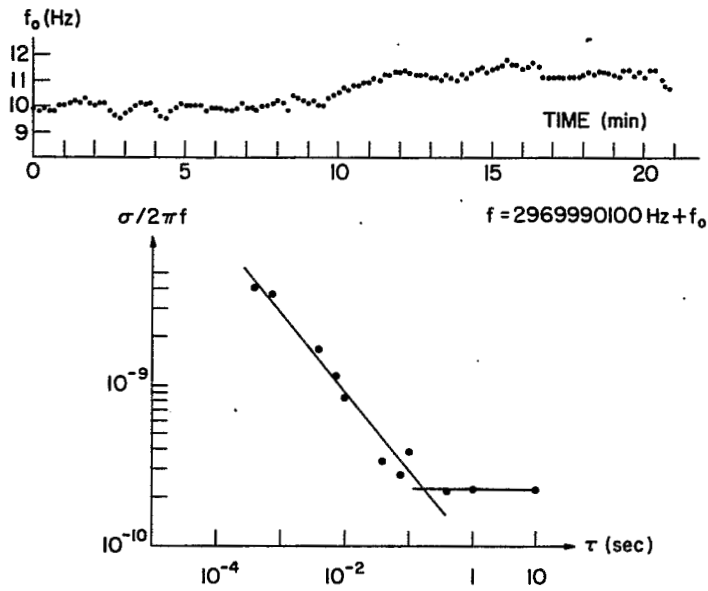


Fig. 5. Oscillator frequency and short-term frequency stability at  $Q = 10^7$ .

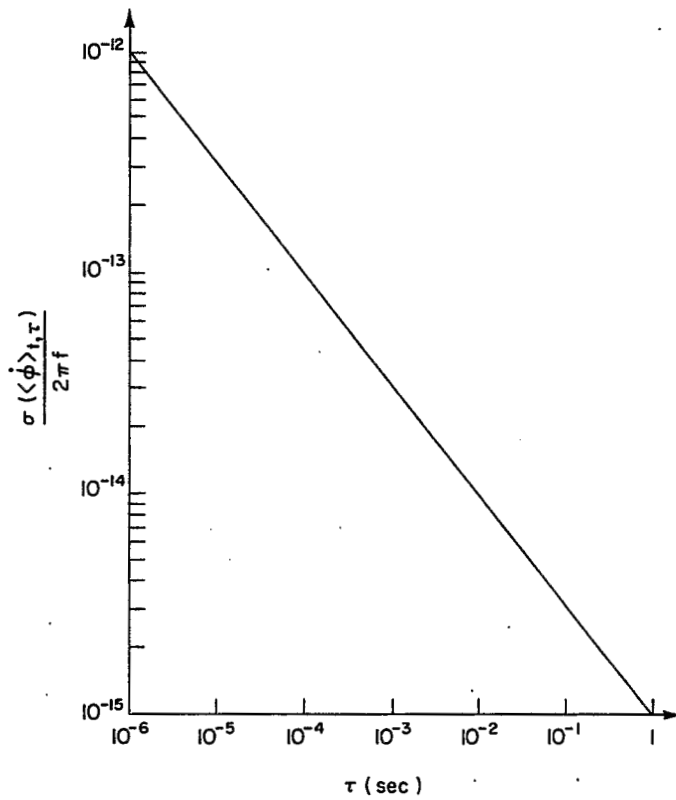


Fig. 6. Theoretical short-term frequency stability:  $f = 3 \text{ GHz}$ ,  $Q = 10^7$ ,  $P = 0.1 \text{ W}$ .

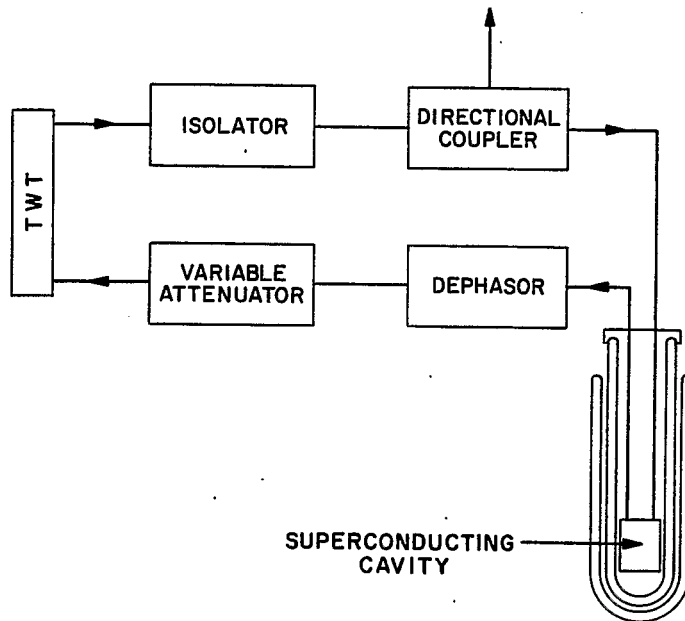


Fig. 7. Block diagram of the TWT auto-oscillator.

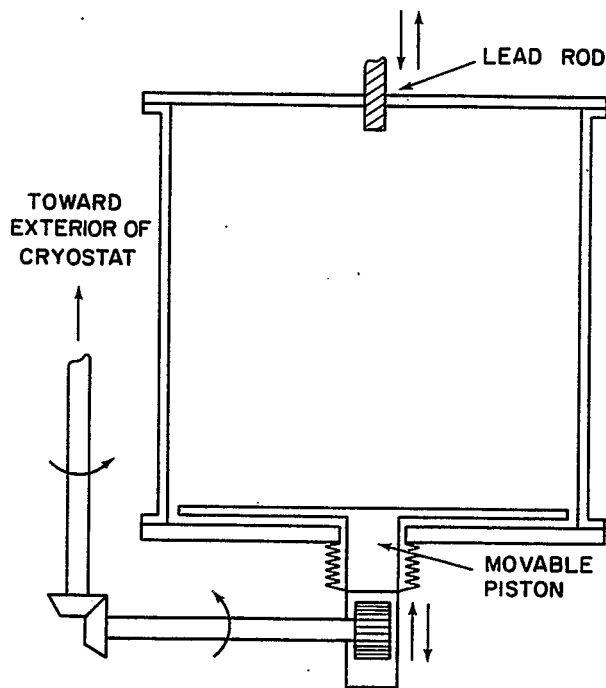


Fig. 8. Tunable cavity.

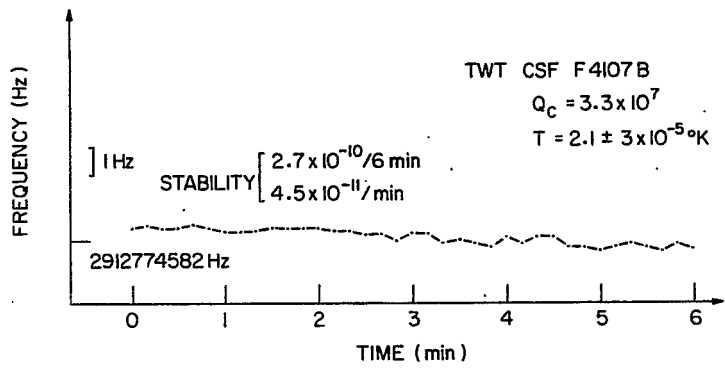


Fig. 9. Frequency vs time.

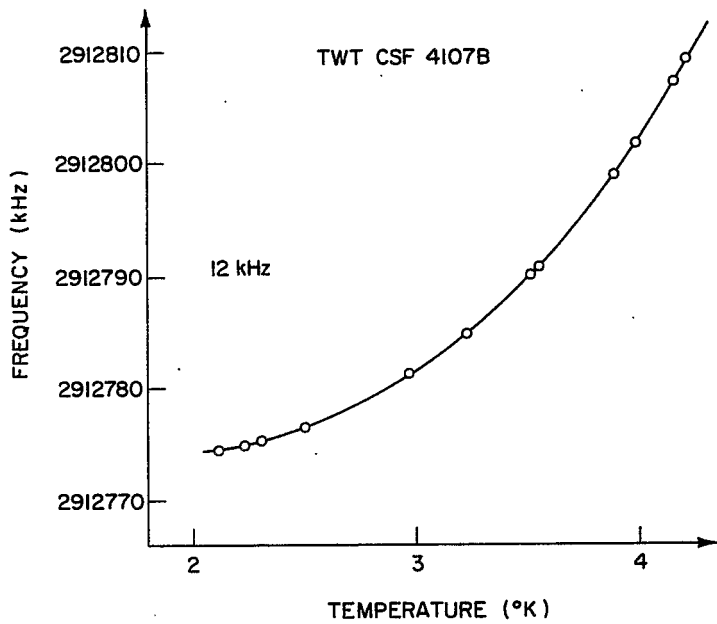


Fig. 10. Frequency vs helium bath temperature.

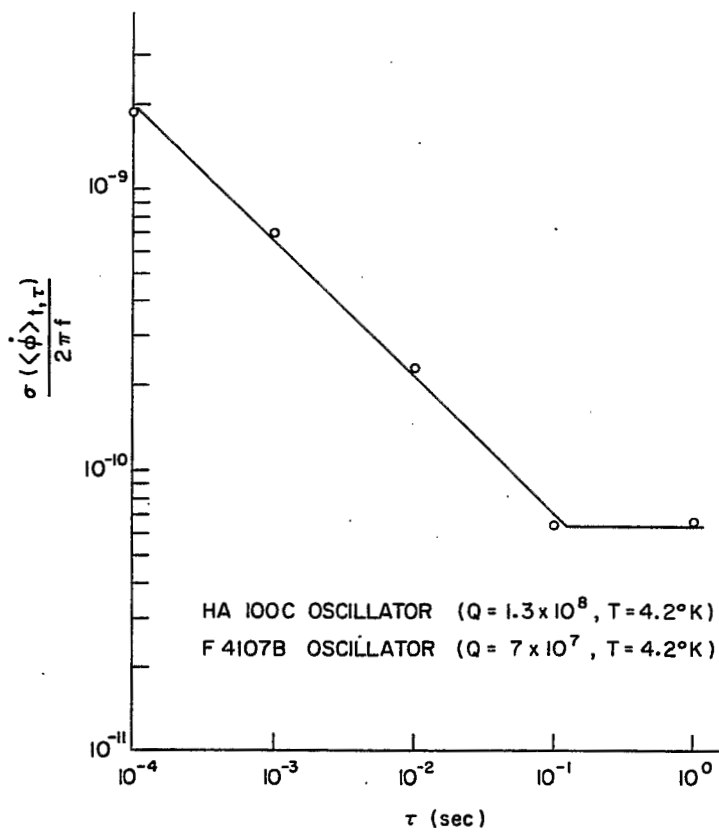


Fig. 11. Short-term frequency stability of TWT oscillator.